Functional Relationship of ATP Hydrolysis, Presynaptic Filament Stability, and Homologous DNA Pairing Activity of the Human Meiotic Recombinase DMC1*

Hao-Yen Chang[‡], **Chia-Yu Liao**[‡], **Guan-Chin Su**[‡], **Sheng-Wei Lin**[§], **Hong-Wei Wang**[¶], and **Peter Chi**[‡§1]

From the [‡]*Institute of Biochemical Sciences, National Taiwan University, Number 1, Section 4, Roosevelt Road, Taipei 10617 Taiwan, the* [§]*Institute of Biological Chemistry, Academia Sinica, 128 Academia Road, Section 2, Nankang, Taipei 11529, Taiwan, and the* [¶]*Ministry of Education Key Laboratory of Protein Science, Tsinghua-Peking Joint Center for Life Sciences, Center for Structural Biology, School of Life Sciences, Tsinghua University, Beijing 100084, China*

Background: DMC1 and RAD51 recombinases catalyze ATP-dependent DNA strand exchange via the presynaptic filament.

Results: Attenuation of ATP hydrolysis correlates with stabilization of the presynaptic filament but does not enhance DMC1 activity.

Conclusion: In contrast to RAD51, stabilization of the presynaptic filament via ATP hydrolysis attenuation is insufficient for enhancement of the DMC1-catalyzed recombination reaction.

Significance: The results reveal an important mechanistic difference between RAD51 and DMC1.

DMC1 and RAD51 are conserved recombinases that catalyze homologous recombination. DMC1 and RAD51 share similar properties in DNA binding, DNA-stimulated ATP hydrolysis, and catalysis of homologous DNA strand exchange. A large body of evidence indicates that attenuation of ATP hydrolysis leads to stabilization of the RAD51-ssDNA presynaptic filament and enhancement of DNA strand exchange. However, the functional relationship of ATPase activity, presynaptic filament stability, and DMC1-mediated homologous DNA strand exchange has remained largely unexplored. To address this important question, we have constructed several mutant variants of human DMC1 and characterized them biochemically to gain mechanistic insights. Two mutations, K132R and D223N, that change key residues in the Walker A and B nucleotide-binding motifs ablate ATP binding and render DMC1 inactive. On the other hand, the nucleotide-binding cap D317K mutant binds ATP normally but shows significantly attenuated ATPase activity and, accordingly, forms a highly stable presynaptic filament. Surprisingly, unlike RAD51, presynaptic filament stabilization achieved via ATP hydrolysis attenuation does not lead to any enhancement of DMC1-catalyzed homologous DNA pairing and strand exchange. This conclusion is further supported by examining wild-type DMC1 with non-hydrolyzable ATP analogues. Thus, our results reveal an important mechanistic difference between RAD51 and DMC1.

Homologous recombination (HR)[2] is indispensable for the maintenance of genomic integrity and also helps create genetic diversity (1–7). To initiate HR, a recombinase enzyme polymerizes on ssDNA derived from the nucleolytic processing of a primary lesion, *e.g.* a DNA double-strand break, to form a right-handed, helical protein filament known as the presynaptic filament. The presynaptic filament searches for homology in duplex DNA, and once homology is located, recombinase-mediated DNA pairing forms a D-loop structure to initiate genetic exchange (1–4).

RAD51 and DMC1 are the two conserved recombinases that catalyze HR reactions in eukaryotes. Although RAD51 functions in both mitotic and meiotic cells, DMC1 is meiosis-specific (8, 9). Genetic studies in the budding yeast have shown that both Rad51 and Dmc1 are essential for the proper execution of meiotic recombination. Recent work has provided evidence that the essential role of Rad51 in meiosis is to enhance the recombinase activity of Dmc1 (10). These results thus reveal distinct functions of Rad51 and Dmc1 in meiotic HR (11–13). In mice, a homozygous deletion of *Rad51* causes embryonic lethality. In contrast, the *Dmc1*$^{-/-}$ mutant is viable although sterile (14–17).

With both RAD51 and DMC1, presynaptic filament formation requires ATP (18–23). In the case of RAD51, ATP hydrolysis by the presynaptic filament leads to the turnover of protein protomers and drives the branch migration of Holliday junctions (24–27). It has been well documented that the attenuation of ATP hydrolysis, either through the introduction of specific mutations into RAD51 or through the use of a non-hydrolyzable ATP analogue, enhances the stability of the presynaptic filament and recombinase activity (28–30). Consistent

[1] To whom correspondence should be addressed: Institute of Biochemical Sciences, College of Life Science, National Taiwan University, No. 1, Sec. 4, Roosevelt Rd., Taipei 10617, Taiwan. Tel.: 886-2-23665573; Fax: 886-2-23635038; Email: peterhchi@ntu.edu.tw.

[2] The abbreviations used are: HR, homologous recombination; AMP-PNP, 5′-adenylyl-β,γ-imidodiphosphate; AMP-PCP, adenosine 5′-(β,γ-methyl-enetriphosphate); ATPγS, adenosine 5′-O-(thiotriphosphate); Oligo, oligonucleotide.

with this relationship, the RAD51-interacting SWI5-SFR1 complex facilitates RAD51-mediated recombination by maintaining the ATP-bound form of the RAD51 presynaptic filament (31, 32). Thus, the active conformation of the RAD51 presynaptic filament requires ATP being bound, but ATP hydrolysis is dispensable and in fact diminishes recombinase activity because of protein turnover. DMC1 also requires ATP for the assembly of a functional presynaptic filament and to perform homologous DNA pairing and strand exchange. However, studies that have been conducted thus far provide no evidence for an up-regulation of DMC1 recombinase activity upon attenuation of ATP hydrolysis by the presynaptic filament (22, 33, 34). These observations suggest important mechanistic differences between RAD51 and DMC1 with regards to presynaptic filament assembly and recombinase activity.

In this study, we have strived to define how ATP hydrolysis affects the stability of the DMC1 presynaptic filament and ensuing homologous DNA pairing and strand exchange efficiency. For this purpose, we have generated the D317K mutant that exhibits attenuated ATPase activity but remains proficient in ATP binding. Our biochemical analyses reveal that although the DMC1 D317K mutant protein readily forms a presynaptic filament with enhanced stability, it is compromised for the ability to mediate homologous DNA pairing and strand exchange. Similar results have been obtained using the non-hydrolyzable ATP analogues AMP-PNP and AMP-PCP with wild-type DMC1. Our findings thus provide evidence that, unlike RAD51, ATP hydrolysis by the DMC1 presynaptic filament correlates with filament stability but not with DNA pairing and strand exchange activity.

Experimental Procedures

DNA Substrates—Both replicative form I dsDNA and viral (+)-strand Φx174 ssDNA were purchased from New England Biolabs. The linear Φx174 dsDNA was prepared by treatment of the replicative form I dsDNA with the restriction enzyme PstI (New England Biolabs) and purification using the PCR purification kit (Qiagen). Oligonucleotides were purified as described previously (31). The 80-mer Oligo 1 (5′-TTA-TGTTCATTTTTTATATCCTTTACTTTATTTTCTCTG-TTTATTCATTTACTTATTTTGTATTATCCTTATCTTA-TTTA) was used to assemble the presynaptic filament for DNA strand exchange reactions. To prepare the homologous 40-mer duplex dsDNA, Oligo 2 (5′-TAATACAAAATAAGTAAATG-AATAAACAGAGAAAATAAAG) was 5′ end-labeled with polynucleotide kinase (New England Biolabs) and [γ-^{32}P]ATP (PerkinElmer). Following removal of the unincorporated nucleotide with a Spin 6 column (Bio-Rad), the radiolabeled oligonucleotide was annealed to its exact complement (Oligo 3) by heating the mixture of the two oligonucleotides at 85 °C for 10 min and its slow cooling to 25 °C over the course of ~1.5 h. After purification from a 10% polyacrylamide gel, the duplex was concentrated. For the D-loop reaction, the 90-mer Oligo 4 (5′-AAATCAATCTAAAGTATATATGAGTAAACTTGGT-CTGACAGTTACCAATGCTTAATCAGTGAGGCACCTAT-CTCAGCGATCTGTCTATTT) was 5′ end-labeled as above. To prepare 5′ end-labeled ssDNA for the Exonuclease I protection assay, Oligo 1 was 5′ end-labeled as above. For the RecJ

protection assay, Oligo 1 was treated with terminal transferase (Roche Applied Science) and [α-^{32}P]dATP (PerkinElmer) to label its 3′ end. The unincorporated nucleotides were removed as above.

Plasmids—The DMC1 expression plasmid was obtained by inserting the human DMC1 cDNA into the BamHI site of the pRSFDuet vector (Novagen), which added a His$_6$ tag to the amino terminus of the protein. Construction of the DMC1 mutant variants D317K, K132R, and D223N was by site-directed mutagenesis. All the protein expression plasmids were sequenced to ensure that no undesired mutation had occurred.

Protein Expression and Purification—RecA-deficient *Escherichia coli* cells (strain BLR) harboring the His$_6$-tagged DMC1 expression plasmid were cultured in Luria broth at 37 °C until the A_{600} reached 0.6–0.8, at which point 1 mM isopropyl-1-thio-β-D-galactopyranoside was added and cultures were incubated for an additional 2.5 h at 37 °C. All the protein purification steps were carried out at 4 °C. To purify the His$_6$-tagged DMC1, 50–60 g of cell paste was suspended in 150 ml of breakage buffer (25 mM Tris-HCl, pH 7.5, 10% glycerol, 300 mM KCl, 0.01% IGEPAL, 2 mM β-mercaptoethanol, 1 mM PMSF, and the protease inhibitors aprotinin, chymostatin, leupeptin, Bestatin, and pepstatin A, each at 3 μg/ml). The cell suspension was then subjected to sonication. The clarified lysate was prepared by centrifugation (100,000 × *g* for 1 h) and incubated with 5 ml of TALON resin (Clontech) for 4 h. The slurry was transferred to a column and washed with 50 ml of breakage buffer containing 5 mM imidazole. DMC1 was eluted with 25 ml of elution buffer (25 mM Tris-HCl, pH 7.5, 10% glycerol, 150 mM KCl, 0.01% IGEPAL, 2 mM β-mercaptoethanol, and 200 mM imidazole) containing protease inhibitors. The eluate was fractionated in a 1-ml Source Q column by applying a 60-ml gradient of 75–450 mM KCl in buffer A (25 mM Tris-HCl, pH 7.5, 10% glycerol, 0.01% IGEPAL, 2 mM β-mercaptoethanol, and 0.5 mM EDTA). The pooled DMC1-containing fraction was diluted and further fractionated in a 1-ml macrohydroxyapatite column using a 45-ml gradient of 70–630 mM KH$_2$PO$_4$ in buffer A containing 75 mM KCl. The pooled DMC1-containing fraction was diluted and further fractionated in a 1-ml Mono Q column with a 30-ml 75–400 mM KCl gradient in buffer A. Then, the DMC1-containing fractions were pooled and concentrated in a Centricon-30 concentrator (Millipore). The concentrated preparation was divided into small aliquots and stored at −80 °C. The His$_6$-tagged DMC1 D317K, His$_6$-tagged DMC1 K132R, and His$_6$-tagged DMC1 D223N were expressed and purified using the same procedure.

UV Cross-linking Assay—A previously described procedure was followed (35). Briefly, His$_6$-tagged DMC1 or mutant protein was incubated with 2.4 μCi of [γ-^{32}P]ATP in buffer B (35 mM Tris-HCl, pH 7.5, 1 mM DTT, 100 ng/μl BSA, 100 mM KCl, and 5 mM MgCl$_2$) for 10 min at 37 °C, and cross-linking was carried out using a Stratalinker® UV Crosslinker 1800 (Stratagene) for 10 min on ice. Samples were resolved by 13.5% SDS-PAGE at 4 °C, and the gel was dried onto DE81 Paper (Whatman) and analyzed in the Personal Molecular Imager (PMI) (Bio-Rad).

ATPase Assay—His$_6$-tagged DMC1 or DMC1 D317K (2.5 μM) was incubated in buffer C (35 mM Tris-HCl, pH 7.5, 1 mM
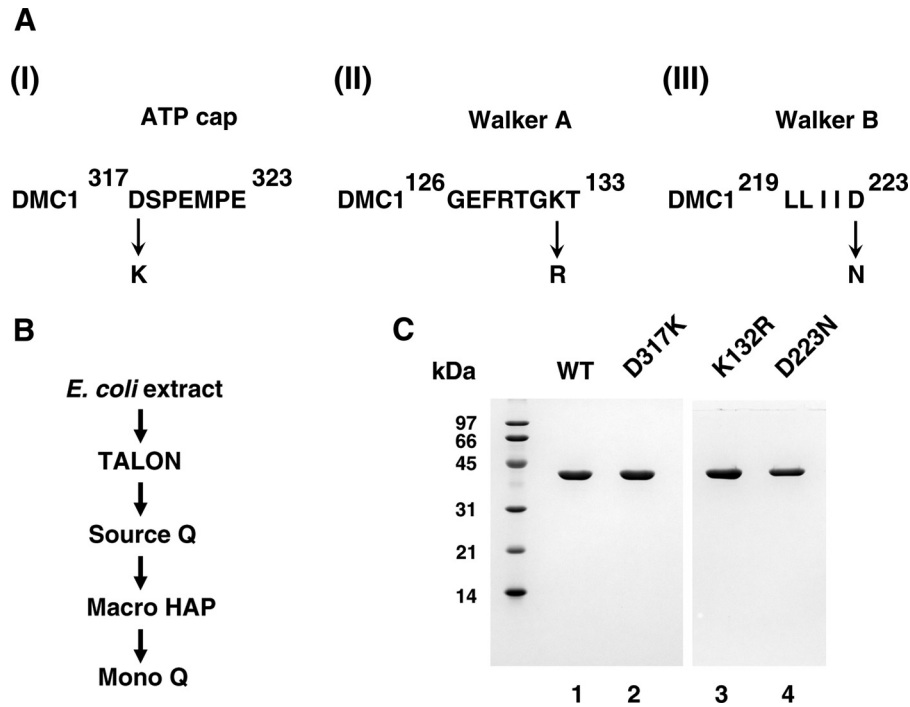
FIGURE 1. **Purification of human DMC1 and mutant proteins.** *A*, the conserved aspartate (Asp-317) residue in the ATP cap of human DMC1 was mutated to lysine, as indicated (*panel I*). The conserved lysine (Lys-132) residue in the Walker A motif was changed to arginine (*panel II*), and the conserved aspartate (Asp-223) residue in the Walker B motif was changed to asparagine (*panel III*). *B*, protein purification procedure. *C*, purified wild-type DMC1 (*WT, lane 1*), DMC1 D317K (*lane 2*), DMC1 K132R (*lane 3*), and DMC1 D223N (*lane 4*) proteins, 3 μg each, were analyzed on a 15% denaturing polyacrylamide gel with Coomassie Blue staining.

DTT, 100 ng/μl BSA, 15 mM KCl, 5 mM MgCl$_2$, 1 mM ATP, and 0.6 μCi of [γ-^{32}P]ATP without or with Φx174 viral (+) strand ssDNA (37.5 μM nucleotides) or linearized dsDNA (37.5 μM base pairs) at 37 °C for the indicated times. Aliquots (2 μl) were taken at the indicated times and mixed with an equal volume of 500 mM EDTA. ATP hydrolysis was determined by thin-layer chromatography on a polyethyleneimine sheet (Sigma-Aldrich) using 0.15 M LiCl and 0.5 M formic acid as the developing buffer. The chromatography sheet was air-dried and subjected to phosphorimaging analysis.

DNA Mobility Shift Assay—The Φx174 viral (+) strand ssDNA (15 μM nucleotides) or linearized dsDNA (15 μM base pairs) was incubated with the indicated amount of His$_6$-tagged DMC1 or DMC1 D317K in 10 μl of buffer B (35 mM Tris-HCl, pH 7.5, 1 mM DTT, 100 ng/μl BSA, 100 mM KCl and 5 mM MgCl$_2$) with 1 mM ATP at 37 °C for 5 min. Reaction mixtures fractionated in a 1% agarose gel in TAE buffer (40 mM Tris, 20 mM acetate, pH 7.5, and 2 mM EDTA) at 4 °C, and the DNA species were stained with ethidium bromide. The gels were analyzed in a gel documentation station (Bio-Rad). For Fig. 3*C*, the 5′ end ^{32}P-labeled 80-mer Oligo 1 ssDNA (3 μM nucleotides) were incubated with the indicated amount of His$_6$-tagged DMC1 or DMC1 D317K in 10 μl of buffer B with 1 mM nucleotide (ATP, AMP-PNP, or AMP-PCP) at 37 °C for 5 min. The reaction mixtures were fractionated in 4% non-denaturing polyacrylamide gels in TAE buffer at 4 °C. The gels were dried onto DE81 paper and subjected to phosphorimaging analysis.

Exonuclease Protection Assay—For this assay, His$_6$-tagged DMC1 or DMC1 D317K was incubated with either 5′ or 3′ ^{32}P-labeled Oligo 1 ssDNA (3 μM nucleotides) in 9 μl of buffer B (35 mM Tris-HCl, pH 7.5, 1 mM DTT, 100 ng/μl BSA, 100 mM KCl and 5 mM MgCl$_2$) with 1 mM nucleotide (ATP, AMP-PNP, or AMP-PCP, as indicated) at 37 °C for 5 min. Then, *E. coli* Exonuclease I, which has a 3′ to 5′ polarity and was used to test the 5′ end-labeled DNA (0.8 unit; New England Biolabs), or *E. coli* RecJ, which has a 5′ to 3′ polarity and was used to test the 3′ end-labeled DNA, was added to the reaction mixture (10 μl final volume). After 5 min of digestion at 37 °C, reaction mixtures were mixed with 2.5 μl of termination buffer (240 mM EDTA, 0.2% SDS, and proteinase K at 0.32 mg/ml) and incubated at 37 °C for 15 min. Then, the reaction mixtures were resolved in a 10% polyacrylamide gel in TBE buffer (89 mM Tris, 89 mM borate, and 2 mM EDTA, pH 8.0), and after drying the gel, the DNA species were quantified by phosphorimaging analysis.

DNA Strand Exchange Assay—The 80-mer Oligo 1 (4.8 μM nucleotides) was incubated with the indicated amount of His$_6$-tagged DMC1 or DMC1 D317K in buffer B (35 mM Tris-HCl, pH 7.5, 1 mM DTT, 100 ng/μl BSA, 100 mM KCl, and 5 mM MgCl$_2$) with 1 mM nucleotide (ATP, ADP, ATPγS, AMP-PNP, or AMP-PCP, as indicated) for 5 min at 37 °C. The reaction was initiated by adding homologous ^{32}P-labeled 40-mer duplex (2.4 μM base pairs) to a final volume of 12.5 μl. After a 30-min incubation, a 5-μl aliquot was removed, mixed with an equal volume of 0.1% SDS containing proteinase K (1 mg/ml), and incubated at 37 °C for 15 min. The samples were fractionated in 10% polyacrylamide gels in TBE buffer. Gels were dried onto DE81 paper and subjected to phosphorimaging analysis.

D-loop Assay—The ^{32}P-labeled 90-mer Oligo 4 (2.4 μM nucleotides) was incubated with the indicated amount of His$_6$-
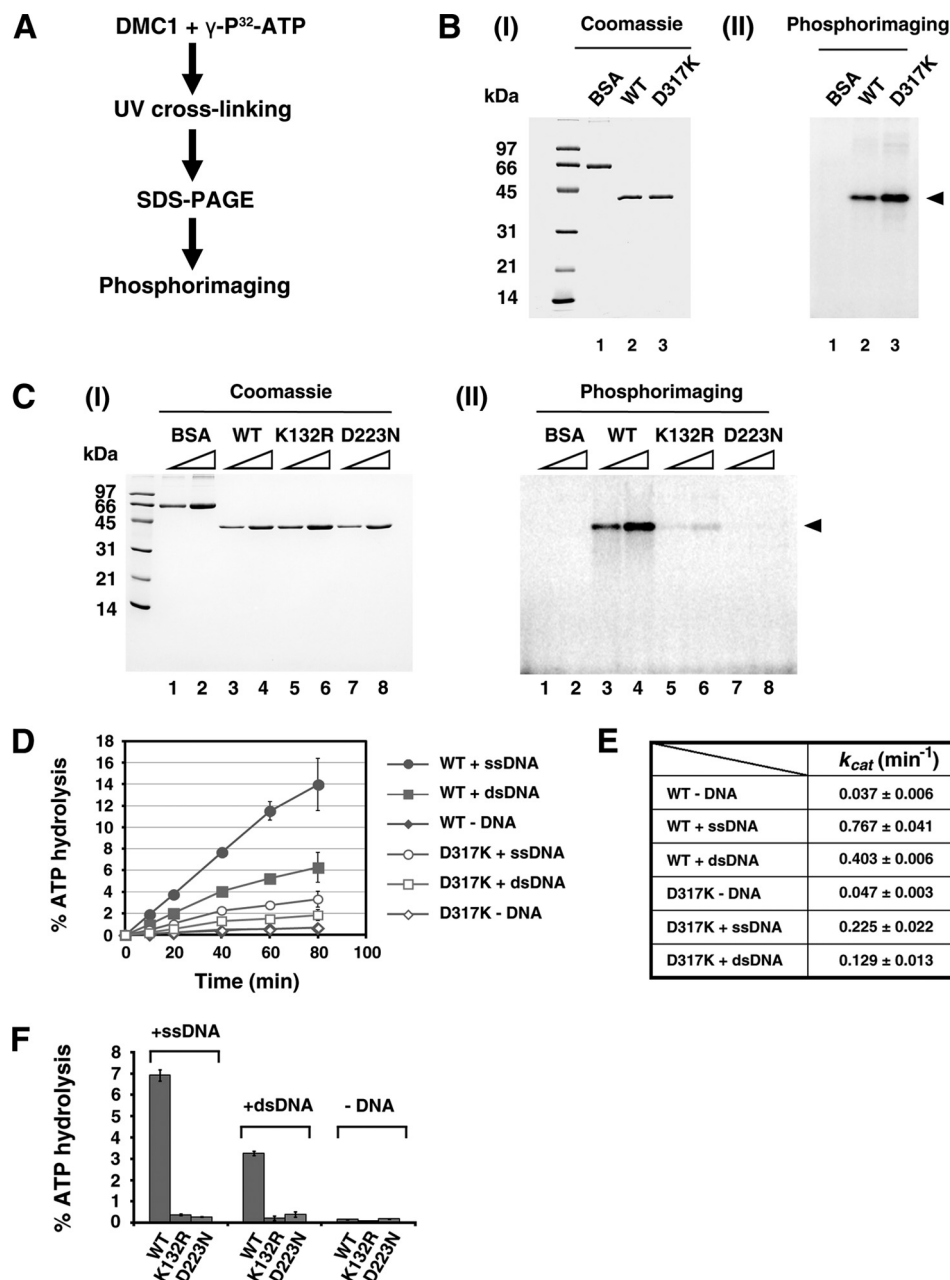
FIGURE 2. **ATP binding and hydrolysis by DMC1 and mutant proteins.** *A*, schematic of the UV cross-linking analysis. DMC1 and mutant proteins were incubated with [γ-^{32}P]ATP. Following UV cross-linking, radiolabeled proteins were run on a 13.5% denaturing polyacrylamide gel and visualized by phosphorimaging. *B*, wild-type DMC1 (*WT*), DMC1 D317K, and BSA (2.4 μM each) were treated as described in *A* and then analyzed by 13.5% SDS-PAGE and Coomassie Blue staining (*panel I*) and in the Personal Molecular Imager (PMI) (*panel II*). *C*, the ATP binding property of DMC1 K132R and D223N (2.4 and 4.8 μM each) was examined by SDS-PAGE and Coomassie Blue staining (*panel I*) and in the Personal Molecular Imager (PMI) (*panel II*). *D*, DMC1 D317K exhibits attenuated ATPase activity. Briefly, wild-type DMC1 (*WT*) and DMC1 D317K were incubated with [γ-^{32}P]ATP without DNA (− *DNA*), with circular Φx174 DNA (+ *ssDNA*), or with Φx174 replicative form DNA (+ *dsDNA*) for the indicated times. *E*, DMC1 k_{cat} values are estimated from levels of ATP hydrolysis at the 40-min time point. *F*, wild-type DMC1 (*WT*), DMC1 K132R, and DMC1 D223N were examined for ATP hydrolysis. *D* and *F*, *error bars* represent the ± S.D. calculated from three independent experiments.

tagged DMC1 or DMC1 D317K in 10.5 μl of buffer B (35 mM Tris-HCl, pH 7.5, 1 mM DTT, 100 ng/μl BSA, 100 mM KCl, and 5 mM MgCl$_2$) with 1 mM nucleotide (ATP, ADP, ATPγS, AMP-PNP, or AMP-PCP, as indicated) for 5 min at 37 °C. The reaction was initiated by adding pBluescript replicative form I DNA (190 μM base pairs) to a 12.5-μl final volume. After 4 min of incubation, a 5-μl aliquot was removed, mixed with an equal volume of 0.1% SDS containing proteinase K (1 mg/ml), and incubated at 37 °C for 15 min. The samples were

analyzed on 0.9% agarose gels in TBE buffer at 4 °C. Gels were dried onto DE81 paper and subjected to phosphorimaging analysis.

Results

Construction of DMC1 Mutants—Although ATP is required for DMC1-mediated homologous DNA pairing and strand exchange (34), the role of ATP hydrolysis in the reaction remains uncertain. To address this issue, we aimed to identify
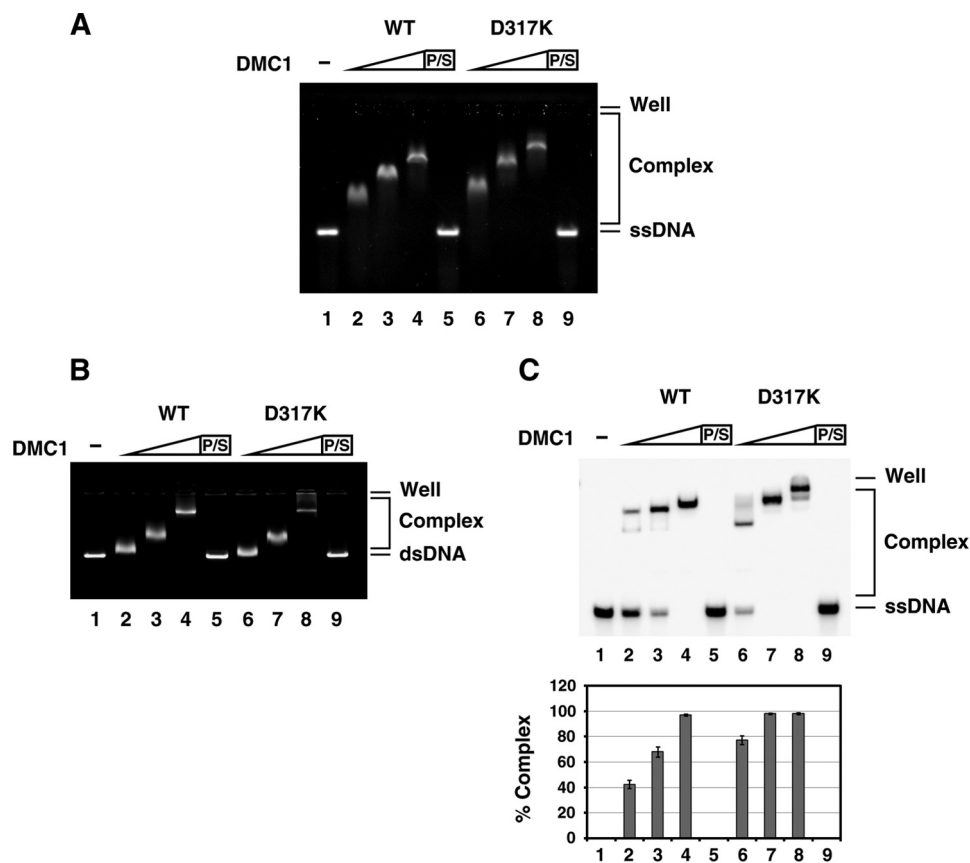
FIGURE 3. **DNA binding activity of DMC1 and DMC1 D317K.** *A* and *B*, wild-type DMC1 (*WT*) and DMC1 D317K (*lanes 2* and *6*, 1.25 μM; *lanes 3* and *7*, 2.5 μM; *lanes 4*, *5*, *8*, and *9*, 7.5 μM) were incubated with circular Φx174 ssDNA (15 μM nucleotides, in *A*) or linear Φx174 dsDNA (15 μM base pairs, in *B*). The DNA species were resolved in a 1% agarose gel and stained with ethidium bromide. Treatment of the nucleoprotein complex with proteinase K and SDS (*P/S*) released the DNA substrate (*lanes 5* and *9*). *C*, DMC1 (*WT*) and DMC1 D317K (*lanes 2* and *6*, 0.5 μM; *lanes 3* and *7*, 1 μM; *lanes 4*, *5*, *8*, and *9*, 3 μM) were incubated with ^{32}P-labeled 80-mer ssDNA (3 μM nucleotides). The DNA species were revealed in a 4% polyacrylamide gel, which was dried and subjected to phosphorimaging analysis. The results were graphed, and the *error bars* represent the $\pm$ S.D. based on at least three independent experiments.

DMC1 mutant variants that bind ATP but exhibit attenuated ATP hydrolysis. To this end, we focused on residues in DMC1 (namely, Asp-317, Lys-132, and Asp-223) predicted to affect ATP hydrolysis based on the following rationale. (*a*) We changed Asp-317 in the ATP cap in DMC1 to Lys (Fig. 1*A*, *panel I*) because mutating the analogous residue in RAD51 has no effect on ATP binding ability but greatly attenuates ATP hydrolysis (30). (*b*) Lys-132 in DMC1, part of the Walker A motif involved in ATP binding, was changed to Arg because the equivalent mutation in other ATPases (28) often affects ATP hydrolysis without a significant effect on ATP binding (Fig. 1*A*, *panel II*). (*c*) Asp-223, part of the Walker B motif in DMC1, was mutated to Asn (Fig. 1*A*, *panel III*) because the equivalent mutation in several AAA+ ATPases ablates ATP hydrolysis without a strong effect on ATP binding (36–38). DMC1 and the three DMC1 mutants (*i.e.* D317K, K132R, and D223N) were expressed in *E. coli* and purified to near homogeneity. The chromatographs are shown (Fig. 1*B*), and the procedural details were described under "Experimental Procedures." The mutants could be expressed to the same level as the wild-type protein and purified with the same procedure and a similar yield. We obtained wild-type and mutant DMC1 proteins with purities ≥98% (Fig. 1*C*).

The DMC1 D317K Mutant Is Attenuated for ATP Hydrolysis—We first examined the ATP binding ability of the DMC1 mutant variants. Briefly, purified DMC1 and mutants were incubated with [γ-^{32}P]ATP and then irradiated in a Stratalinker® UV Crosslinker 1800. Samples were resolved by SDS-PAGE and analyzed in a Personal Molecular Imager (PMI) (Fig. 2*A*). As shown in Fig. 2*B*, D317K has a more enhanced ATP binding capacity than the wild-type protein (Fig. 2*B*). However, the K132R and D223N variants were significantly impaired for ATP binding (Fig. 2*C*). We next used thin-layer chromatography to examine the mutant DMC1 proteins for their ATPase activity in the presence of either ssDNA or dsDNA. The results showed that D317K is significantly reduced for ATP hydrolysis capability with both DNA species (Fig. 2, *D* and *E*), whereas the K132R and D223N mutants are quite defective in this regard (Fig. 2*F*). The results thus revealed that DMC1 D317K mutant is proficient in ATP binding but specifically impaired for ATP hydrolysis.

DNA Binding Properties of the DMC1 D317K Mutant—It has been documented that DMC1-mediated ATP hydrolysis is stimulated by DNA (20, 34), so it is important to determine whether the reduced activity of DMC1 D317K in ATP hydrolysis might stem from a defect in DNA binding, We used an electrophoretic mobility shift assay to analyze the DNA binding
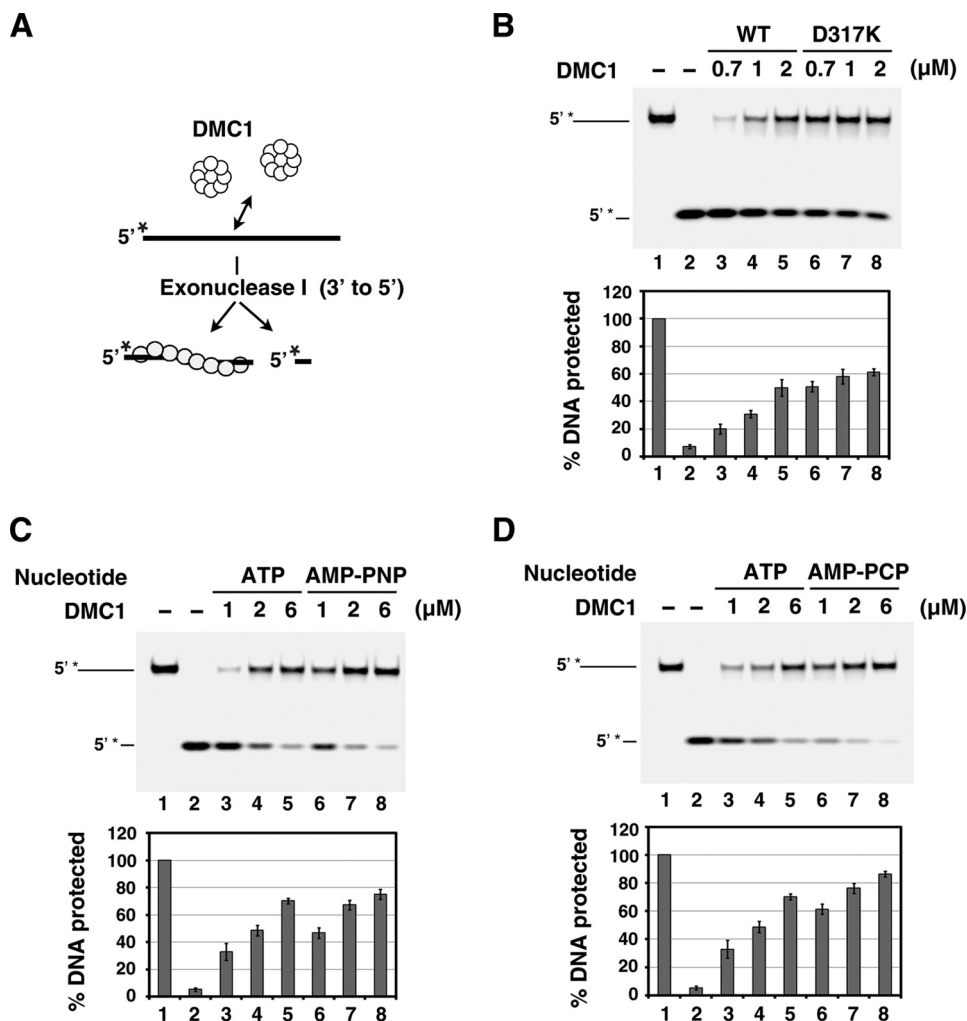
FIGURE 4. **Determination of DMC1 presynaptic filament stability by protection against Exonuclease I.** *A*, schematic of the Exonuclease I protection assay. The 5′ ^{32}P-labeled 80-mer ssDNA (3 μM nucleotides) was incubated with DMC1 before Exonuclease I was added. The reactions were deproteinized and analyzed. The ^{32}P label is denoted by the *asterisk*. *B–D*, the indicated amounts of wild-type DMC1 (*WT*) and DMC1 D317K were analyzed with 1 mM ATP (*B–D*), AMP-PNP (*C*), or AMP-PCP (*D*) as cofactor. The results were graphed, and the *error bars* represent the ± S.D. based on at least three independent experiments.

activity of DMC1 D317K alongside the wild-type protein. The two proteins were incubated with ΦX174 ssDNA (Fig. 3*A*) and also linear dsDNA (Fig. 3*B*) in the presence of ATP, and DNA binding was analyzed in an agarose gel with ethidium bromide staining of the DNA species. Especially with ssDNA, the D317K variant generated a more pronounced shift of the DNA than did wild-type DMC1, suggesting that it has the same or perhaps even an enhanced DNA binding capability (Fig. 3*A*, comparing *lanes 2*, *3*, and *4* with *lanes 6*, *7*, and *8*, respectively). To facilitate quantification of DNA binding, a ^{32}P-labeled 80-mer ssDNA was also employed as the substrate. This allowed us to verify that the D317K variant indeed possesses a higher level of DNA binding activity relative to the wild-type protein (Fig. 3*C*). Taken together, the results above show that the DMC1 D317K mutation affects ATP hydrolysis but leads to an enhanced capability to bind ATP and DNA.

Relationship between ATP Hydrolysis and Presynaptic Filament Stability—The results shown above revealed that attenuating ATP hydrolysis by the D317K mutation is accompanied by an increase in the affinity for DNA. We investigated presyn-

aptic filament stability by incubating the D317K variant with ATP or incubating the wild-type DMC1 with a non-hydrolyzable ATP analogue (AMP-PNP or AMP-PCP). For this, we assembled the DMC1 presynaptic filament on 5′-radiolabeled 80-mer ssDNA and then added *E. coli* Exonuclease I that digests ssDNA with a 3′ to 5′ polarity (Fig. 4*A*) but is prevented from acting by the DMC1 presynaptic filament that shields the DNA. With this method, we found that the DMC1 D317K mutant forms a presynaptic filament with increased stability relative to wild-type DMC1 (Fig. 4*B*). As expected, the presynaptic filament of wild-type DMC1 was stabilized when AMP-PNP (Fig. 4*C*) or AMP-PCP (Fig. 4*D*) was used as the nucleotide cofactor.

We also examined the protection of a 3′-radiolabeled ssDNA against the action of RecJ, a 5′ to 3′ exonuclease, to rule out any potential role of polarity in filament growth or dissociation (Fig. 5*A*). As shown in Fig. 5*B*, the DMC1 D317K mutant again afforded a greater degree of protection of the ssDNA than did the wild-type protein, again indicative of an enhanced stability of the presynaptic filament that harbored the DMC1 mutant
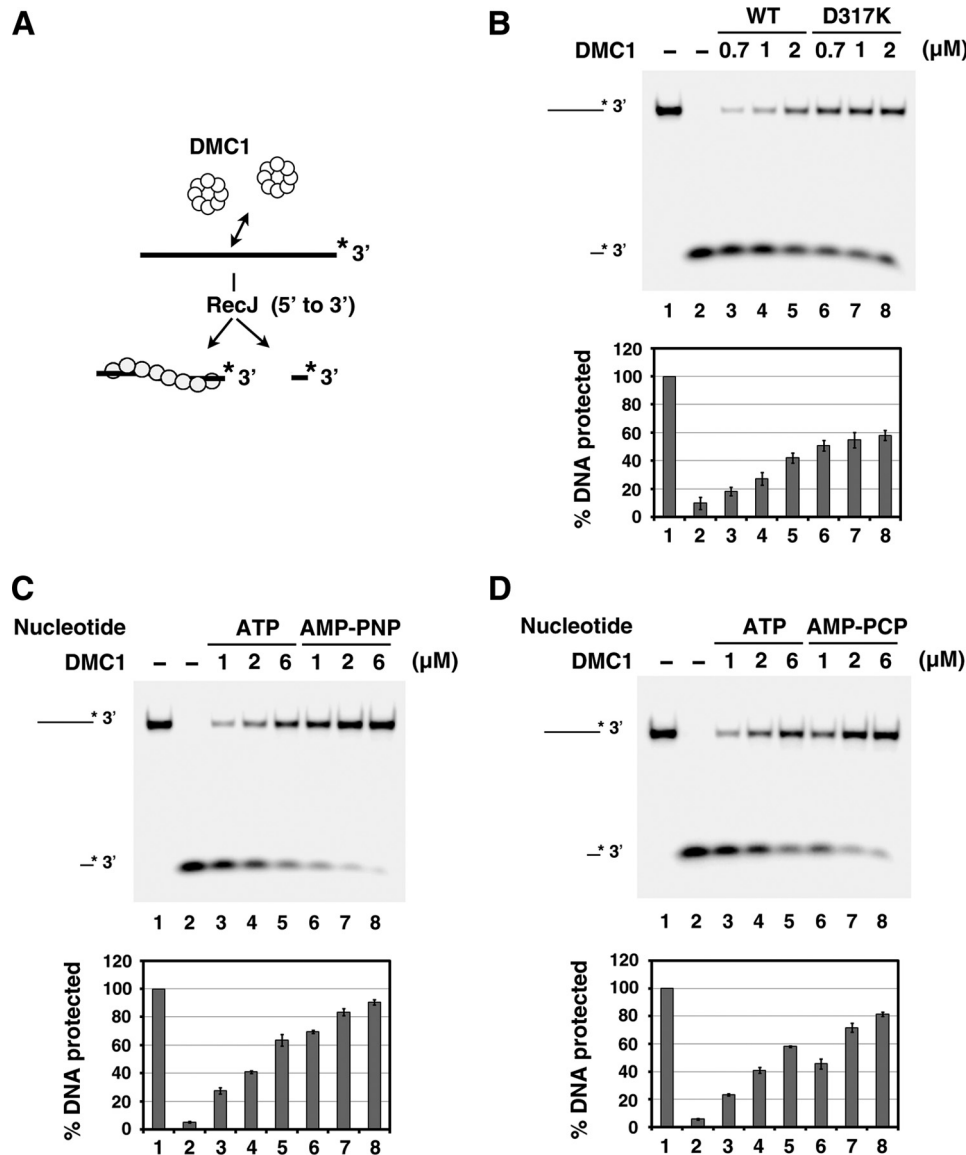
FIGURE 5. **Determination of DMC1 presynaptic filament stability by protection against RecJ.** *A*, schematic of the RecJ protection assay. The 3' ^{32}P-labeled 80-mer ssDNA (3 μM nucleotides) was incubated with DMC1 before RecJ was added. The reactions were deproteinized and analyzed. The ^{32}P label is denoted by the *asterisk*. *B–D*, wild-type DMC1 (*WT*) and DMC1 D317K were analyzed with 1 mM ATP (*B–D*), AMP-PNP (*C*), or AMP-PCP (*D*) as cofactor. The results were graphed, and the *error bars* represent the ± S.D. based on at least three independent experiments.

(Fig. 5*B*). Just as in the Exonuclease I assay, AMP-PNP and AMP-PCP enhanced the filament stability of wild-type DMC1 (Fig. 5, *C* and *D*). We note that neither wild-type nor the mutant DMC1 was able to protect ssDNA against digestion by Exonuclease I or RecJ without a nucleotide co-factor (data not shown). Taken together, the results above revealed that attenuation of the ATPase activity of DMC1 leads to enhanced stability of the presynaptic filament.

Dependence of DMC1-mediated Homologous DNA Pairing on ATP Hydrolysis—Attenuation of ATP hydrolysis by the RAD51 presynaptic filament leads to filament stabilization and an enhanced ability of the filament to mediate DNA strand exchange (28–30). We examined whether the increase in DMC1 presynaptic filament stability also facilitates DNA strand exchange. We used the DNA strand exchange system depicted in Fig. 6*A* to address this issue. Surprisingly, unlike

RAD51, the presynaptic filament consisting of the DMC1 D317K variant has a diminished level of DNA strand exchange activity as compared with its wild-type counterpart (Fig. 6*B*). Moreover, wild-type DMC1 shows no enhancement but, rather, a slight decrease in DNA strand exchange activity when AMP-PNP or AMP-PCP was used instead of ATP as the nucleotide cofactor (Fig. 6*C*).

We next used the D-loop assay to further investigate the relationship between presynaptic filament stability and the recombinase activity of DMC1. In this assay, we monitored the assimilation of a radiolabeled 90-mer ssDNA into pBluescript plasmid DNA, as depicted in Fig. 7*A*. The results showed that DMC1 D317K is less capable than the wild-type protein in D-loop formation (Fig. 7*B*). Moreover, in the nucleotide substitution experiment with wild-type DMC1, we found (*a*) little or
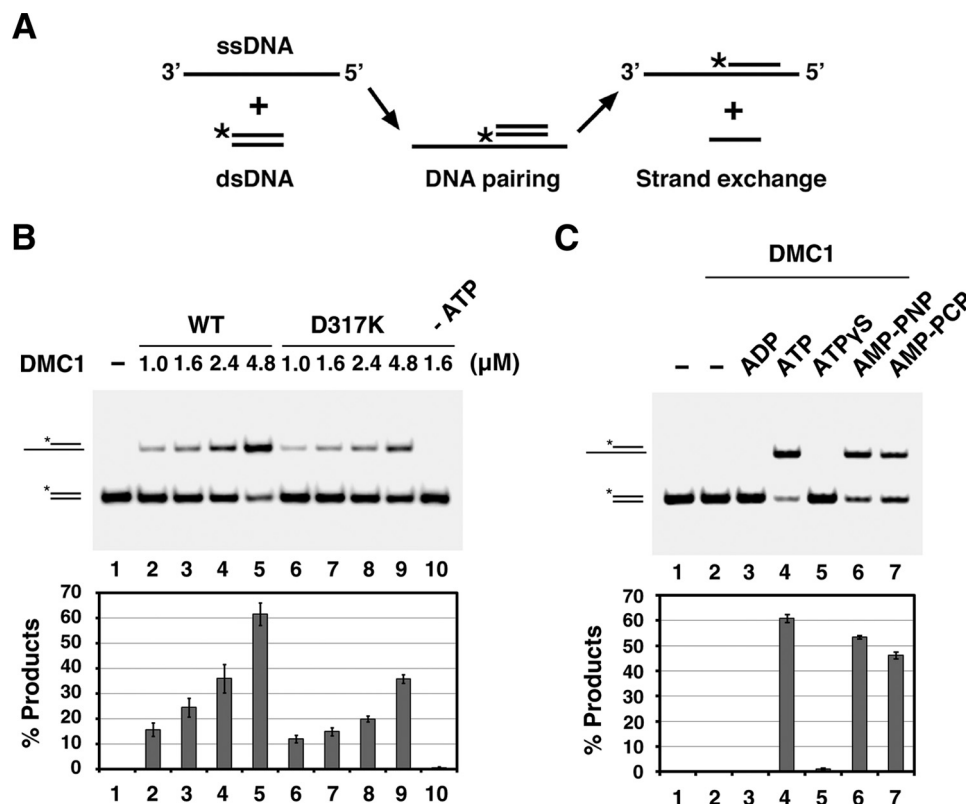
FIGURE 6. **DNA strand exchange in the absence of ATP hydrolysis.** *A*, schematic of the DNA strand exchange assay. The ssDNA was incubated with DMC1 followed by the addition of ^{32}P-labeled dsDNA. The reactions were deproteinized and analyzed. The ^{32}P label is denoted by the *asterisk*. *B* and *C*, the DNA strand exchange activity of wild-type DMC1 (*WT*) and DMC1 D317K was analyzed with 1 mM ATP (*B* and *C*) or the indicated nucleotide (*C*) as cofactor. The results were graphed, and the *error bars* represent the ± S.D. based on at least three independent experiments.

no D-loop product with either ADP or ATPγS and (*b*) a slight decrease in D-loop formation with AMP-PNP or AMP-PCP as compared with ATP (Fig. 7*C*) (see Refs. 33 and 34 and this study). We note that the D317K variant is unable to execute D-loop formation using AMP-PNP or AMP-PCP as the nucleotide cofactor (data not shown). Taken together, the results provide evidence that, in contrast to RAD51, an increase in DMC1 filament stability does not necessarily lead to the enhancement of homologous DNA pairing and strand exchange.

Discussion

Dependence of the DMC1 Recombinase Activity on ATP Binding and Hydrolysis—To investigate the functional relationship among ATP hydrolysis, presynaptic filament stability, and homologous DNA pairing and strand exchange activity for DMC1, we sought to identify DMC1 mutant variants that are capable of binding ATP but exhibit attenuated ATP hydrolysis. In this regard, we have constructed and tested the D317K, K132R, and D223N mutant variants. We note that neither the K132R nor the D223N variant is capable of ATP binding. Accordingly, these mutants also lack the ability to form a functional presynaptic filament as revealed by their failure to protect ssDNA against Exonuclease I challenge or to perform DNA strand exchange (34) (Fig. 8). On the other hand, the D317K mutant fulfills the stated criteria, in that it is proficient in ATP binding but is significantly impaired for ATP hydrolysis. We have demonstrated that DMC1 D317K forms a more stable

nucleoprotein filament than its wild-type counterpart. Surprisingly, this does not lead to any enhancement of homologous DNA pairing and strand exchange *in vitro*. In congruence with this, we have furnished evidence that wild-type DMC1 forms a highly stable presynaptic filament with the non-hydrolyzable ATP analogue AMP-PNP or AMP-PCP, but, in this case also, filament stabilization does not enhance DNA pairing and strand exchange. In conclusion, attenuation of DMC1 ATPase activity promotes the stability of the presynaptic filament but is insufficient to stimulate, and may even reduce, DNA pairing and strand exchange.

Differences in Functional Attributes between RAD51 and DMC1—We have summarized previous findings and our current results regarding the biochemical properties of wild-type and mutant RAD51 and DMC1 proteins, including their ATPase activity, presynaptic filament assembly, and homologous DNA pairing and strand exchange activity, in Table 1 (see Refs. 28–30 and the present work). There are clear parallels between the two recombinases. Specifically, both RAD51 and DMC1 require ATP to form a functional presynaptic filament, and the attenuation of ATP hydrolysis leads to filament stabilization in both cases. Interestingly, although ATP hydrolysis attenuation enhances the stability of presynaptic filaments of RAD51 and DMC1, the increased stability facilitates RAD51-mediated homologous DNA pairing and strand exchange but has no stimulatory effect on the DMC1-catalyzed reaction *in vitro* (Table 1). We note that the RAD51 presynaptic filament, upon hydrolyzing ATP, accumulates ADP and becomes converted to an inactive form, whereas the DMC1 filament does
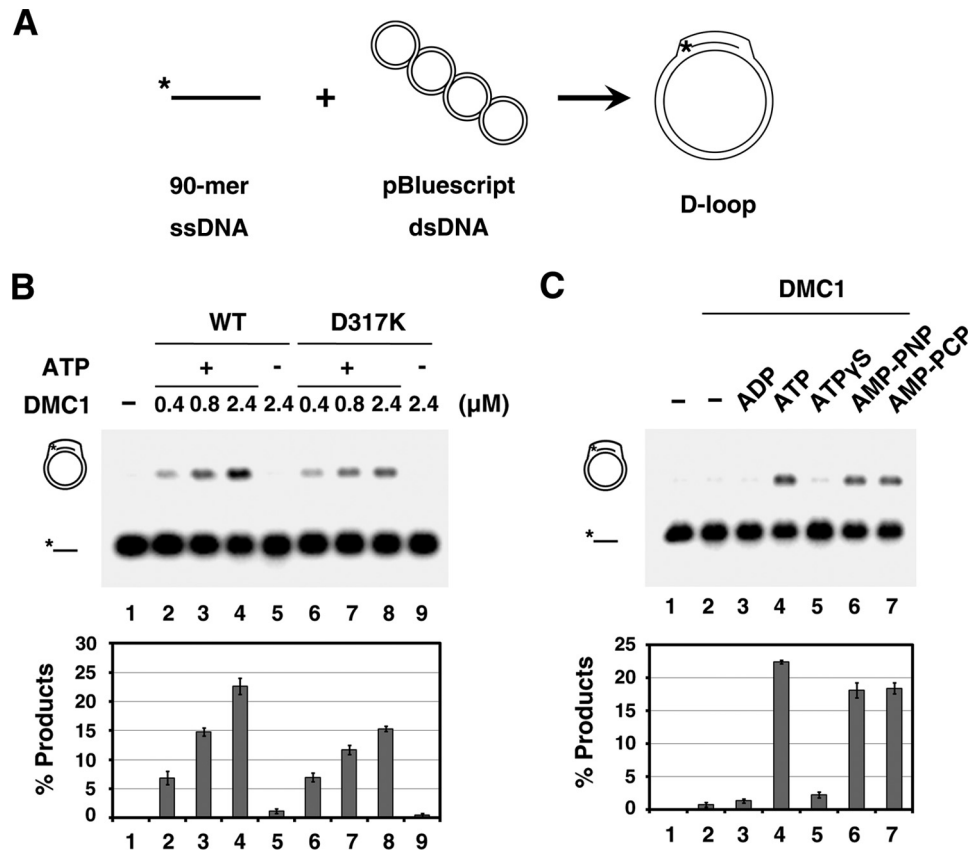
FIGURE 7. **D-loop formation in the absence of ATP hydrolysis.** *A*, schematic of the D-loop assay. The ^{32}P-labeled 90-mer ssDNA was incubated with DMC1 followed by the addition of the pBluescript dsDNA. The ^{32}P label is denoted by the *asterisk*. *B* and *C*, the ability of wild-type DMC1 (*WT*) and DMC1 D317K to form D-loops was analyzed with 1 mM ATP (*B* and *C*) and the indicated nucleotide (*C*) as cofactor. The results were graphed, and the *error bars* represent the ± S.D. based on at least three independent experiments.
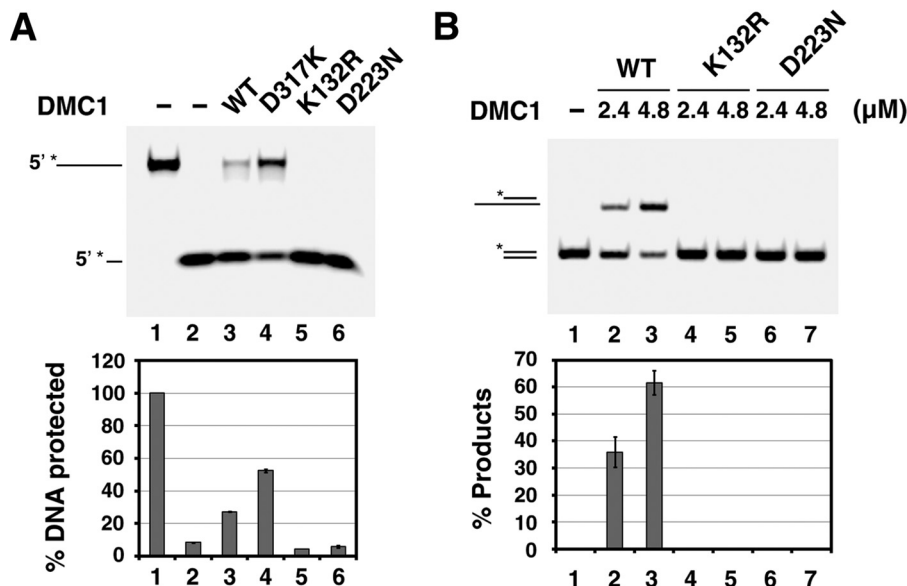

FIGURE 8. **Defects of the DMC1 K132R and D223N mutants in presynaptic filament formation and DNA strand exchange.** *A*, wild-type DMC1 (*WT*) and the D317K, K132R, and D223N mutants were examined for presynaptic filament formation by the Exonuclease I protection assay as in Fig. 4. The ^{32}P label is denoted by the *asterisk*. *B*, the ability of wild-type DMC1 (*WT*) and the K132R and D223N mutants to catalyze DNA strand exchange was examined as in Fig. 6. The results were graphed in *A* and *B*, and the *error bars* represent the ± S.D. calculated based on at least three independent experiments.

not undergo such inactivation when ATP is hydrolyzed (29, 33). This biochemical difference between RAD51 and DMC1 could account for the differential stimulation of RAD51-mediated DNA strand exchange when ATP hydrolysis is attenuated. In summary, unlike RAD51, enhanced presynaptic filament stability via ATP hydrolysis attenuation does not lead to any enhancement of DMC1-catalyzed homologous DNA pairing and strand exchange.

Mutants	Functions	RAD51 ATP hydrolysis	RAD51-ssDNA Stability	RAD51 Strand-exchange	DMC1 ATP hydrolysis	DMC1-ssDNA Stability	DMC1 Strand-exchange
D317→K	ATP-cap	< WT	> WT	> WT	< WT	> WT	< WT
K132→R	Walker A	< WT	> WT	> WT	—[#]	—	—
D223→N	Walker B	ND	ND	ND	—[#]	—	—
ATP Analogues	**Mechanism**	**RAD51 ATP hydrolysis**	**RAD51-ssDNA Stability**	**RAD51 Strand-exchange**	**DMC1 ATP hydrolysis**	**DMC1-ssDNA Stability**	**DMC1 Strand-exchange**
AMP-PNP	P_β-P_γ restricted	—	> WT+ATP	> WT+ATP	—	> WT+ATP	< WT+ATP
AMP-PCP	P_β-P_γ restricted	—	ND	ND	—	> WT+ATP	< WT+ATP

[#] DMC1-K132R and DMC1-D223N are defective in ATP binding.

As stated above, our results suggest that stabilization of the DMC1 presynaptic filament does not necessarily stimulate the DMC1-catalyzed HR reaction. It is important to note, however, that several studies have provided a positive correlation between presynaptic filament stability and the recombinase activity of DMC1. Most notably, it has been found that the DMC1 accessory factor HOP2-MND1 stimulates DMC1 activity partly by stabilizing the presynaptic filament (39, 40). One plausible explanation is that HOP2-MND1, in addition to stabilizing the presynaptic filament, also triggers a conformational change of DMC1 protomers within the presynaptic filament to facilitate DMC1-mediated homologous DNA pairing and strand exchange. The premise is supported by a recent study showing that HOP2-MND1 promotes conversion of the RAD51 presynaptic filament to the active conformation to facilitate DNA strand exchange (41).

In addition, Mazin and colleagues (29, 33) have found that calcium increases the stability of the presynaptic filament and the recombinase activity of both RAD51 and DMC1. Interestingly, the stimulatory effects of RAD51 and DMC1 by Ca^{2+} are different mechanistically. In the case of RAD51, the inhibition of ATP hydrolysis by Ca^{2+} enhances presynaptic filament stability and recombinase activity. Importantly, the Ca^{2+} dependence can be bypassed by the addition of AMP-PNP, strongly suggesting that Ca^{2+} up-regulates RAD51 activity by stabilizing the presynaptic filament (29). In marked contrast, a similar stimulation of DMC1 activity by Ca^{2+} is observed even in the presence of AMP-PNP with wild-type DMC1 or in the presence of ATP with DMC1 D317K (33).[3] These results suggest that Ca^{2+} stimulates the DMC1-catalyzed HR reaction by inducing a conformational change in the recombinase (33). Taken together, these results strongly suggest that the active conformation of DMC1 may be achieved via the addition of Ca^{2+} or an appropriate accessory factor (2, 33, 39). It will be important in the future to determine the active conformation of the DMC1 presynaptic filament and to examine how accessory factors induce the requisite conformational change.

Author Contributions—P. C. conceived and coordinated the study. H. Y. C., and P. C. wrote the paper. H. Y. C., C. Y. L., G. C. S., and S. W. L. performed and analyzed the experiments. H. W. W. provided technical assistance and contributed to the preparation of the figures. All authors reviewed the results and approved the final version of the manuscript.

References

1. Krogh, B. O., and Symington, L. S. (2004) Recombination proteins in yeast. *Annu. Rev. Genet.* **38,** 233–271
2. San Filippo, J., Sung, P., and Klein, H. (2008) Mechanism of eukaryotic homologous recombination. *Annu. Rev. Biochem.* **77,** 229–257
3. Heyer, W. D., Ehmsen, K. T., and Liu, J. (2010) Regulation of homologous recombination in eukaryotes. *Annu. Rev. Genet.* **44,** 113–139
4. Moynahan, M. E., and Jasin, M. (2010) Mitotic homologous recombination maintains genomic stability and suppresses tumorigenesis. *Nat. Rev. Mol. Cell Biol.* **11,** 196–207
5. Aguilera, A., and García-Muse, T. (2013) Causes of genome instability. *Annu. Rev. Genet.* **47,** 1–32
6. Malkova, A., and Haber, J. E. (2012) Mutations arising during repair of chromosome breaks. *Annu. Rev. Genet.* **46,** 455–473
7. Cole, F., Keeney, S., and Jasin, M. (2012) Preaching about the converted: how meiotic gene conversion influences genomic diversity. *Ann. N.Y. Acad. Sci.* **1267,** 95–102
8. Neale, M. J., and Keeney, S. (2006) Clarifying the mechanics of DNA strand exchange in meiotic recombination. *Nature* **442,** 153–158
9. Sehorn, M. G., and Sung, P. (2004) Meiotic recombination: an affair of two recombinases. *Cell Cycle* **3,** 1375–1377
10. Cloud, V., Chan, Y. L., Grubb, J., Budke, B., and Bishop, D. K. (2012) Rad51 is an accessory factor for Dmc1-mediated joint molecule formation during

meiosis. *Science* **337,** 1222–1225

11. Hong, S., Sung, Y., Yu, M., Lee, M., Kleckner, N., and Kim, K. P. (2013) The logic and mechanism of homologous recombination partner choice. *Mol. Cell* **51,** 440–453

12. Lao, J. P., Cloud, V., Huang, C. C., Grubb, J., Thacker, D., Lee, C. Y., Dresser, M. E., Hunter, N., and Bishop, D. K. (2013) Meiotic crossover control by concerted action of Rad51-Dmc1 in homolog template bias and robust homeostatic regulation. *PLoS Genet.* **9,** e1003978

13. Hayase, A., Takagi, M., Miyazaki, T., Oshiumi, H., Shinohara, M., and Shinohara, A. (2004) A protein complex containing Mei5 and Sae3 promotes the assembly of the meiosis-specific RecA homolog Dmc1. *Cell* **119,** 927–940

14. Tsuzuki, T., Fujii, Y., Sakumi, K., Tominaga, Y., Nakao, K., Sekiguchi, M., Matsushiro, A., Yoshimura, Y., and Morita, T. (1996) Targeted disruption of the *Rad51* gene leads to lethality in embryonic mice. *Proc. Natl. Acad. Sci. U.S.A.* **93,** 6236–6240

15. Yoshida, K., Kondoh, G., Matsuda, Y., Habu, T., Nishimune, Y., and Morita, T. (1998) The mouse *RecA*-like gene *Dmc1* is required for homologous chromosome synapsis during meiosis. *Mol. Cell* **1,** 707–718

16. Pittman, D. L., Cobb, J., Schimenti, K. J., Wilson, L. A., Cooper, D. M., Brignull, E., Handel, M. A., and Schimenti, J. C. (1998) Meiotic prophase arrest with failure of chromosome synapsis in mice deficient for *Dmc1*, a germline-specific RecA homolog. *Mol. Cell* **1,** 697–705

17. Lim, D. S., and Hasty, P. (1996) A mutation in mouse *rad51* results in an early embryonic lethal that is suppressed by a mutation in p53. *Mol. Cell Biol.* **16,** 7133–7143

18. Sheridan, S. D., Yu, X., Roth, R., Heuser, J. E., Sehorn, M. G., Sung, P., Egelman, E. H., and Bishop, D. K. (2008) A comparative analysis of Dmc1 and Rad51 nucleoprotein filaments. *Nucleic Acids Res.* **36,** 4057–4066

19. Yu, X., and Egelman, E. H. (2010) Helical filaments of human Dmc1 protein on single-stranded DNA: a cautionary tale. *J. Mol. Biol.* **401,** 544–551

20. Li, Z., Golub, E. I., Gupta, R., and Radding, C. M. (1997) Recombination activities of HsDmc1 protein, the meiotic human homolog of RecA protein. *Proc. Natl. Acad. Sci. U.S.A.* **94,** 11221–11226

21. Gupta, R. C., Golub, E., Bi, B., and Radding, C. M. (2001) The synaptic activity of HsDmc1, a human recombination protein specific to meiosis. *Proc. Natl. Acad. Sci. U.S.A.* **98,** 8433–8439

22. Sehorn, M. G., Sigurdsson, S., Bussen, W., Unger, V. M., and Sung, P. (2004) Human meiotic recombinase Dmc1 promotes ATP-dependent homologous DNA strand exchange. *Nature* **429,** 433–437

23. Baumann, P., Benson, F. E., and West, S. C. (1996) Human Rad51 protein promotes ATP-dependent homologous pairing and strand transfer reactions in vitro. *Cell* **87,** 757–766

24. Fung, C. W., Fortin, G. S., Peterson, S. E., and Symington, L. S. (2006) The *rad51-K191R* ATPase-defective mutant is impaired for presynaptic filament formation. *Mol. Cell Biol.* **26,** 9544–9554

25. Li, X., Zhang, X. P., Solinger, J. A., Kiianitsa, K., Yu, X., Egelman, E. H., and Heyer, W. D. (2007) Rad51 and Rad54 ATPase activities are both required to modulate Rad51-dsDNA filament dynamics. *Nucleic Acids Res.* **35,** 4124–4140

26. Sigurdsson, S., Van Komen, S., Petukhova, G., and Sung, P. (2002) Homologous DNA pairing by human recombination factors Rad51 and Rad54. *J. Biol. Chem.* **277,** 42790–42794

27. Rossi, M. J., Mazina, O. M., Bugreev, D. V., and Mazin, A. V. (2011) The RecA/RAD51 protein drives migration of Holliday junctions via polymerization on DNA. *Proc. Natl. Acad. Sci. U.S.A.* **108,** 6432–6437

28. Chi, P., Van Komen, S., Sehorn, M. G., Sigurdsson, S., and Sung, P. (2006) Roles of ATP binding and ATP hydrolysis in human Rad51 recombinase function. *DNA Repair (Amst.)* **5,** 381–391, 10.1016/j.dnarep.2005.11.005

29. Bugreev, D. V., and Mazin, A. V. (2004) Ca^{2+} activates human homologous recombination protein Rad51 by modulating its ATPase activity. *Proc. Natl. Acad. Sci. U.S.A.* **101,** 9988–9993

30. Amunugama, R., He, Y., Willcox, S., Forties, R. A., Shim, K. S., Bundschuh, R., Luo, Y., Griffith, J., and Fishel, R. (2012) RAD51 protein ATP cap regulates nucleoprotein filament stability. *J. Biol. Chem.* **287,** 8724–8736

31. Tsai, S. P., Su, G. C., Lin, S. W., Chung, C. I., Xue, X., Dunlop, M. H., Akamatsu, Y., Jasin, M., Sung, P., and Chi, P. (2012) Rad51 presynaptic filament stabilization function of the mouse Swi5-Sfr1 heterodimeric complex. *Nucleic Acids Res.* **40,** 6558–6569

32. Su, G. C., Chung, C. I., Liao, C. Y., Lin, S. W., Tsai, C. T., Huang, T., Li, H. W., and Chi, P. (2014) Enhancement of ADP release from the RAD51 presynaptic filament by the SWI5-SFR1 complex. *Nucleic Acids Res.* **42,** 349–358

33. Bugreev, D. V., Golub, E. I., Stasiak, A. Z., Stasiak, A., and Mazin, A. V. (2005) Activation of human meiosis-specific recombinase Dmc1 by Ca^{2+}. *J. Biol. Chem.* **280,** 26886–26895

34. Sharma, D., Say, A. F., Ledford, L. L., Hughes, A. J., Sehorn, H. A., Dwyer, D. S., and Sehorn, M. G. (2013) Role of the conserved lysine within the Walker A motif of human DMC1. *DNA Repair (Amst.)* **12,** 53–62, 10.1016/j.dnarep.2012.10.005

35. Tombline, G., Shim, K. S., and Fishel, R. (2002) Biochemical characterization of the human RAD51 protein. II. Adenosine nucleotide binding and competition. *J. Biol. Chem.* **277,** 14426–14433

36. Rai, V., Gaur, M., Shukla, S., Shukla, S., Ambudkar, S. V., Komath, S. S., and Prasad, R. (2006) Conserved Asp327 of Walker B motif in the N-terminal nucleotide binding domain (NBD-1) of Cdr1p of *Candida albicans* has acquired a new role in ATP hydrolysis. *Biochemistry* **45,** 14726–14739

37. Stratford, F. L., Ramjeesingh, M., Cheung, J. C., Huan, L. J., and Bear, C. E. (2007) The Walker B motif of the second nucleotide-binding domain (NBD2) of CFTR plays a key role in ATPase activity by the NBD1-NBD2 heterodimer. *Biochem. J.* **401,** 581–586

38. Chiraniya, A., Finkelstein, J., O'Donnell, M., and Bloom, L. B. (2013) A novel function for the conserved glutamate residue in the Walker B motif of replication factor C. *Genes (Basel)* **4,** 134–151, 10.3390/genes4020134

39. Zhao, W., Saro, D., Hammel, M., Kwon, Y., Xu, Y., Rambo, R. P., Williams, G. J., Chi, P., Lu, L., Pezza, R. J., Camerini-Otero, R. D., Tainer, J. A., Wang, H. W., and Sung, P. (2014) Mechanistic insights into the role of Hop2-Mnd1 in meiotic homologous DNA pairing. *Nucleic Acids Res.* **42,** 906–917

40. Pezza, R. J., Voloshin, O. N., Vanevski, F., and Camerini-Otero, R. D. (2007) Hop2/Mnd1 acts on two critical steps in Dmc1-promoted homologous pairing. *Genes Dev.* **21,** 1758–1766

41. Bugreev, D. V., Huang, F., Mazina, O. M., Pezza, R. J., Voloshin, O. N., Camerini-Otero, R. D., and Mazin, A. V. (2014) HOP2-MND1 modulates RAD51 binding to nucleotides and DNA. *Nat. Commun.* **5,** 4198